Comprehensive circular RNA expression profile in radiation-treated HeLa cells and analysis of radioresistance-related circRNAs

Duo Yu [1] , **Yunfeng Li** [1] , **Zhihui Ming** [2] , **Hongyong Wang** [1] , **Zhuo Dong** [3] , **Ling Qiu** [1] , **Tiejun Wang** [Corresp. 1]

[1] Radiotherapy Department, 2nd Hospital Affiliated to Jilin University, Changchun, China

[2] Stomatology Department, 1st Hospital Affiliated to Jilin University, Changchun, China

[3] College of Public Medicine, Key laboratory of Radiobiology, Ministry of Health, Jilin University, Changchun, China

Corresponding Author: Tiejun Wang
Email address: wangtiejunyd@sina.com

Background: Cervical cancer is one of the most common cancers in women worldwide. Malignant tumors develop resistance mechanisms and are less sensitive to or do not respond to irradiation.With the development of high-throughput sequencing technologies, circular RNA(circRNA) has been identified in an increasing number of diseases, especially cancers. It has been reported that circRNA can compete with microRNAs (miRNAs) to change the stabilityor translation of target RNAs, thus regulating gene expression at the transcriptional level. However, the role of circRNAs in cervical cancer and the radioresistance mechanisms of HeLa cells are unknown. The objective of this study is to investigate the role of circRNAs in radioresistance in HeLa cells. **Methods:** High-throughput sequencing and bioinformatics analysis of irradiated and sham-irradiated HeLa cells. The reliability of high-throughput RNA sequencing was validated using quantitative real-time polymerase chain reaction (qRT-PCR).The most significant circRNA functions and pathways were selected by Gene Ontology(GO) and Kyoto Encyclopedia of Genes and Genomes(KEGG) analyses. A circRNA–miRNA–target gene interaction network was used to find circRNAs associated with radioresistance. Moreover, a protein–protein interaction network was constructed to identify radioresistance-related hub proteins. **Results**: High-throughput sequencing allowed identifying 16,893 circRNAs involved in the response of HeLa cells to radiation. Compared with the control group, there were 153 differentially expressed circRNAs, of which 76 were up-regulated and 77 were down-regulated. GO covered three domains: biological process (BP), cellular component (CC) and molecular function (MF). The terms assigned to the BP domain were peptidyl-tyrosine dephosphorylation and regulation of cell migration. The identified CC terms were cell–cell adherens junction, nucleoplasm and cytosol, and the identified MF terms were protein binding and protein tyrosine phosphatase activity. The top five KEGG pathways were MAPK

signaling pathway, endocytosis, axon guidance, neurotrophin signaling pathway, and SNARE interactions in vesicular transport.The PPI analysisindicated that 19 proteins might be hub proteins. **Conclusions**: CircRNAs may play a major role in the response to radiation.These findings may improve our understanding of the role of circRNAs in radioresistance in HeLa cells and allow the development of novel therapeutic approaches.

1 **Comprehensive circular RNA expression profile in radiation-treated**

2 **HeLa cells and analysis of radioresistance-related circRNAs**

3 Duo Yu [1], Yunfeng Li [1], Zhihui Ming [3], Hongyong Wang [1], Zhuo Dong [2], Ling Qiu

4 [1], Tiejun Wang [1]

6 [1]Radiotherapy Department, 2nd Hospital Affiliated toJilin University, Changchun ,

7 China

8 [2]College of Public Medicine, Key laboratory of Radiobiology, Ministry of Health,

9 Jilin University, Changchun, China

10 3 Stomatology Department, 1st Hospital Affiliated toJilin University, Changchun ,

11 China

13 **Corresponding Author**:

14 Tiejun Wang,

15 E-mail: wangtiejunyd@sina.com

17 **Abstract:**

18 **Background**: Cervical cancer is one of the most common cancers in women

19 worldwide. Malignant tumors develop resistance mechanisms and are less sensitive

20 to or do not respond to irradiation.With the development of high-throughput

21 sequencing technologies, circular RNA(circRNA) has been identified in an

22 increasing number of diseases, especially cancers. It has been reported that

23 circRNA can compete with microRNAs (miRNAs) to change the stabilityor

24 translation of target RNAs, thus regulating gene expression at the transcriptional

25 level. However, the role of circRNAs in cervical cancer and the radioresistance

26 mechanisms of HeLa cells are unknown. The objective of this study is to

27 investigate the role of circRNAs in radioresistance in HeLa cells.

28 **Methods**: High-throughput sequencing and bioinformatics analysis of irradiated

29 and sham-irradiated HeLa cells. The reliability of high-throughput RNA

30 sequencing was validated using quantitative real-time polymerase chain reaction

31 (qRT-PCR).The most significant circRNA functions and pathways were selected

32 by Gene Ontology(GO) and Kyoto Encyclopedia of Genes and Genomes(KEGG)

33 analyses. A circRNA–miRNA–target gene interaction network was used to find

34 circRNAs associated with radioresistance. Moreover, a protein–protein interaction

35 network was constructed to identify radioresistance-related hub proteins.

36 **Results**: High-throughput sequencing allowed identifying 16,893 circRNAs

37 involved in the response of HeLa cells to radiation. Compared with the control

38 group, there were 153 differentially expressed circRNAs, of which 76 were up-

39 regulated and 77 were down-regulated. GO covered three domains: biological

40 process (BP), cellular component (CC) and molecular function (MF). The terms

41 assigned to the BP domain were peptidyl-tyrosine dephosphorylation and

42 regulation of cell migration. The identified CC terms were cell–cell adherens

43   junction, nucleoplasm and cytosol, and the identified MF terms were protein

44   binding and protein tyrosine phosphatase activity. The top five KEGG pathways

45   were MAPK signaling pathway, endocytosis, axon guidance, neurotrophin

46   signaling pathway, and SNARE interactions in vesicular transport.The PPI

47   analysisindicated that 19 proteins might be hub proteins.

48   **Conclusions:** CircRNAs may play a major role in the response to radiation.These

49   findings may improve our understanding of the role of circRNAs in radioresistance

50   in HeLa cells and allow the development of novel therapeutic approaches.

51

52

53   **INTRODUCTION**

54   Cervical cancer is one of the most common cancers in women worldwide and

55   is responsible for the high mortality of female cancers(Du XL et al., 2012). In

56   recent years, with improvements in radiotherapy, radiochemotherapy after

57   operation is the standard treatment for cervical cancer. However, recurrence and

58   metastasis after radiotherapy remain a major problem in the treatment of locally-

59   advanced cervical cancer(de Freitas et al., 2015; Zhao et al., 2013). Therefore, it is

60   crucial to understand the mechanisms underlying the development of

61   radioresistance to improve the therapeutic effect of radiotherapy in the treatment of

62   cervical cancer.

63   Circular RNAs (circRNAs) are non-coding RNA molecules that compose a

64 RNA class that forms covalent closed-loop structures without 5′-3′polarity(Qu et

65 al., 2015). The development of novel biochemical and computational approaches

66 has focused RNA research on circRNAs. CircRNAs are involved in many human

67 diseases, including cancer(Burd et al., 2010b; Bachmayr-Heyda et al., 2015). Some

68 studies have demonstrated that circRNAs play a major role in the biological

69 function of a network of competing endogenous RNAs. Importantly, circRNAs

70 may compete with micro RNAs (miRNAs) to change the stability and translation

71 of target RNAs, thus regulating gene expression at the transcriptional

72 level(Bachmayr-Heyda et al., 2015; Zhong et al., 2018; Ivanov et al., 2015; Qu et

73 al., 2015). Despite this significant progress, the expression profile, mechanism of

74 action, and biological activity of circRNA have not been completely elucidated.

75   In our study, high-throughput RNA sequencing was used to investigate the

76 differential expression profiles of circRNAs between irradiated HeLa cells and

77 sham-irradiated HeLa cells. The comprehensive analysis of radioresistance-related

78 circRNAs may lay a foundation for future studies on the diagnosis and treatment of

79 cervical cancer.

80 **MATERIALS & METHODS**

81 **HeLa cells and irradiation**

82   HeLa cells were purchased from Procell Life Science and Technology Co. Ltd.

83 (Wuhan, China) with short tandem repeat (STR) qualification report

84 (Supplementary data). The cells were cultured in MEM medium (Gibco, Life

85 Technologies Inc., Grand Island, NY, USA)supplemented with 10% fetal bovine

86 serum (Sigma), 1% antibiotic-antimitotic solution (Gibco, Life Technologies).An

87 X-ray generator (Model X-RAD320i X; Precision X-ray, Inc., North Branford,

88 USA) was used to deliver radiation at a dose rate of 1.020 Gy/min (180 kV; 20

89 mA) for a total dose of 10 Gy in the treatment group(irradiated). The control group

90 (sham-irradiated) did not receive radiation as blank comparison. Each group had

91 three samples.

92 **High-throughput sequencing of circRNAs and differential expression analysis**

93 Total RNA was extracted from each group by using TRIzol reagent (Invitrogen,

94 Carlsbad, USA) following the manufacturer's protocol. RNA quantity and quality

95 were determined in a Nano Drop ND-1000 spectrophotometer (Nano Drop

96 Technologies, Inc., Wilmington, USA). RNA integrity was evaluated by standard

97 denaturing agarose gel electrophoresis using the Agilent 2100 Bioanalyzer. The

98 total RNA was measured in a spectrophotometer at the wavelengths of 260 nm and

99 280 nm. The samples with an OD 260/280 ratio of approximately 2.0 were used.

100 CircRNAs were quantitatively analyzed by Novogene Bioinformatics Technology

101 Co.Ltd (Beijing, China). After removal of ribosomal RNA and building a library,

102 high-throughput RNA sequencing was performed. Find_circ was used to identify

103 circRNAs(Memczak et al., 2013). Differentially expressed circRNAs were

104 detected by the negative binomial distribution test using the DESeq2 package. Two

105 criteria were chosen: (i) |log2(foldchange)|>1 and (ii) *P*-value (*P*<0.05).

106 **Construction of the circRNA–miRNA–target gene interaction network**

107   Mounting evidence has indicated that circRNAs may regulate the activity of

108 miRNAs by acting as competing endogenous RNAs or miRNA sponges. The role

109 of circRNAs in HeLa cells subjected to radiation was determined by building a

110 circRNA–miRNA–target gene co-expression network. We used the top four down-

111 regulated and top four up-regulated circRNAs to construct this network using

112 Cytoscape software version 3.2.1. Putative interactions between miRNAs and

113 circRNAs were evaluated using miRanda(3.3a). The top five (highest targeting

114 relationship score) miRNAs were selected, and the target genes of these miRNAs

115 were predicted using miRDB(http://www.mirdb.org). Target scores>98 were

116 selected to construct the circRNA–miRNA–mRNA interaction network.

117 **GO and KEGG pathway analysis**

118   The Gene Ontology (GO) analysis provides a controlled terminology to

119 describe gene and gene product attributes for many organisms. In this study,

120 DAVID (https://david.ncifcrf.gov/) was used to analyze the potential function of

121 target genes. P-values<0.05 were considered statistically significant. GO covers

122 three domains: biological process(BP), cellular component(CC), and molecular

123 function(MF). The five most enriched GO terms were ranked by p-value. KEGG

124 pathway analysis was conducted to determine the involvement of target genes in

125 different biological pathways. DAVID (https://david.ncifcrf.gov/) was also used in

126 this part of the analysis.

Protein–protein interaction(PPI) network analysis

The online tool STRING (https://string-db.org) was used to analyze the target genes. The selection criterion was the highest confidence (interaction score>0.9). Cytoscape software version 3.2.1 was used to draw the PPI network. The hub proteins were selected by their association with other proteins. The target genes with more associations have important roles in the PPI interaction network.

Analysis of the expression level of circRNAs using qRT-PCR

The reliability of high-throughput RNA sequencing was validated. The top four up-regulated circRNAs and top four down-regulated circRNAs were selected. qRT-PCR was performed using Q SYBR green Supermix (Bio Rad), and PCR-specific amplification was conducted in the 7900 HT Sequence Detection System (ABI PRISM, USA). The expression was determined by using the threshold cycle (Ct), and relative expression levels were calculated via the $2^{-\Delta\Delta Ct}$ method. *GAPDH* served as the standard internal control and all reactions were performed in triplicate.

Results

Expression pattern of circRNAs during the priming phase of radiation-treated HeLa cells

High-throughput sequencing was used to determine the expression profile of circRNAs. Two groups of HeLa cells were used, and each group contained three samples. The correlation between gene expression levels in different samples

148 indicated the biological repetition (Figure 1A). The analysis of sequencing data

149 allowed identifying 16,893 circRNAs in HeLa cells. The length of HeLa circRNA

150 candidates ranged from <150 to 99,934 nucleotides (nt). Approximately 67% of

151 circRNAs had the predicted spliced length of < 10,000 nt, whereas 46.4% and 32.0%

152 of the circRNAs had a length of <5,000 and 10,000–50,000 nt, respectively (Figure

153 1B). Among the 16,893 circRNAs, 11,456 were detected in the control group,

154 11,018 were detected in the treatment group, and 5,581 were detected in both

155 groups. The hierarchical clustering showed the gene expression patterns of the

156 samples (Figures 1 C and D.).

Identification of differentially-expressed circRNAs in Hela cells

158 The $\log_2$ (foldchange)|>1 and p-value (p<0.05) were used to evaluate significant

159 differences in the expressions of circRNAs between the two groups. A total of 153

160 circRNAs were differentially expressed in the Treatment Group compared with the

161 Control Group. Of these, the volcano plot indicated that 76 circRNAs were up-

162 regulated and 77 were down-regulated (Figure 1E). The novel genomic feature of

163 circRNAs in both groups is shown in Figure 1F.

Validation of circRNA expression

165 To verify the high-throughput sequencing results, the top four up-regulated and

166 top four down-regulated circRNAs were selected and their expression levels were

167 validated by qRT-PCR analysis. The qRT-PCR results are shown in Figure 2.

168 hsa_circ_0009035, hsa_circ_0000392, hg38_circ_0004913, hsa_circ_0004015

169 were significantly up-regulated in the Treatment Group compared with the Control

170 Group, whereas hg38_circ_0013682, hg38_circ_0015954, hsa_circ_0013738, and

171 hsa_circ_0013225 were down-regulated in the Treatment Group. The expression

172 patterns of these eight circRNAs determined by qRT-PCR agreed with the results

173 of the high-throughput sequencing analysis. The sequence of the primers used in

174 qRT-PCR is shown in Table 1.

175 **Construction of the circRNA–miRNA–target gene interaction network**

176 A circRNA–miRNA–target gene co-expression network was constructed to

177 evaluate the potential functions of circRNAs. Cytoscape was used to draw the

178 circRNA–miRNA–target gene interaction network (Figure 3). It is of interest that

179 circRNAs may play a central role in this interaction network, and a single circRNA

180 may correlate with many miRNAs and regulate many target genes. This network

181 may help elucidate the potential function of circRNAs and their mechanism of

182 action.

183 **GO and KEGG analysis of target genes**

184 The role of circRNAs in response to radiation was investigated by performinga

185 GO functional analysis. The target genes from the circRNA-miRNA-target gene

186 interaction network were used in this analysis. GO has three different

187 domains:biological process (BP), cellular component (CC), and molecular function

188 (MF). The top five(ranked by p-value) BP terms, CC terms, and MF terms are

189 shown in Figure 4 and Table 2. The identified BP terms were peptidyl-tyrosine

190 dephosphorylation, regulation of cell migration, positive regulation of transcription

191 from RNA polymerase II promoter, angiogenesis, and morphogenesis of an

192 epithelial sheet. The identified CC terms were cell–cell adherens junction,

193 nucleoplasm, cytosol, lamellipodium, and nucleus. The identified MF terms were

194 protein binding, tyrosine phosphatase activity, cadherin binding involved in cell-

195 cell adhesion, RNA polymerase II core promoter proximal region sequence-

196 specific DNA binding, transcriptional activator activity, and RNA polymerase II

197 core promoter proximal region sequence-specific binding. The top five(ranked by

198 gene count) KEGG pathways are shown in Figure 5and Table 3. The identified

199 pathways were MAPK signaling, endocytosis, axon guidance, neurotrophin

200 signaling, and SNARE interactions in vesicular transport. It is of note that five

201 genes—*RPS6KA5, RPS6KA6, CRKL, RAP1A, FASLG, MAPK8*—were found in

202 both the MAPK and neurotrophin signaling pathway.

203 **PPI network**

204 STRING was used to predict protein interactions between the target genes.

205 Interaction scores higher than 0.9 (highest confidence) were selected for

206 constructing PPI networks (Figure 6). Nineteen proteins—IGF2R, DNAJC6, FZD4,

207 CBL, CLTC, ARPC3, VAMP2, ITGB3, VAMP4, ITGB1, MAPK8, KIF2A,

208 CLASP1, SMC3, STAG2, STAG1, H2AFZ, RBBP4, and UBE2D3—were

209 strongly correlated with other proteins (connected with > 10 proteins). These hub

210 proteins might play a crucial role in the radioresistance of cervical cancer.

DISCUSSION

211

212   The development of high-throughput sequencing technology has increased our

213   understanding of the role of circRNAs. A recent study found that circRNAs are

214   important members of the non-coding RNA family in different species. The role of

215   circRNA in human disease, especially in cancer, is vital. The functions and

216   biological characteristics of circRNAs may help elucidate the mechanisms

217   underlying human disease. Radioresistance is considered a severe complication of

218   cervical cancer radiotherapy, and the radioresistance mechanism remains poorly

219   understood. In this study, circRNA sequencing was used to analyze the circRNA

220   expression profile between irradiated HeLa cells and sham-irradiated HeLa cells

221   and explore the possible involvement of differentially-expressed circRNAs in

222   radioresistance mechanisms.

223   In the present study, a 10Gy X-ray was applied to HeLa cells, which were

224   collected 48 h later. This interval was chosen because most highly-expressed

225   radiation resistance-related genes are strongly inhibited by radiation after 48h(Shen

226   et al., 2017b; Ghosh & Krishna, 2012b; Balkwill, 2004; Zhang et al., 2017). High-

227   throughput RNA sequencing allowed identifying 16,893 circRNAs in both

228   Treatment and Control Group. A total of 153 circRNAs was differentially

229   expressed (p<0.05, |log2(foldchange)|>1). Four up-regulated and four down-

230   regulated circRNAs validated by qRT-PCR were significantly dysregulated, and

231   this result is consistent with the high-throughput sequencing, indicating the high

Manuscript to be reviewed

232   reliability of high-throughput sequencing data.

233   A circRNA–miRNA–target gene interaction network was constructed to

234   further investigate the regulatory role of circRNAs in radioresistance. This

235   network showed that circRNAs might play a central regulatory role. A single

236   circRNA may be associated with many miRNAs and then may regulate more

237   target genes. For instance, in our study, hsa_circ_0004015 may bind to hsa-miR-

238   3163, hsa-miR-3065-5p, hsa-miR-551b-5p, hsa-miR-4311, and hsa-miR-875-3p.

239   In turn, these miRNAs may be associated with 380 target genes, including *ZYX,*

240   *PRKAR1A, BTAF1, LRP3*, and*ETS1*.

241   The potential regulatory role of circRNAs in radioresistance was further

242   investigated by conducting KEGG and GO analyses and determining the

243   differential expression of mRNAs in the two study groups. GO analysis was

244   performed to annotate the BPs, CCs, and MFs of target genes. The GO analysis

245   results indicated that the high expression of target genes might be involved in cell

246   migration and angiogenesis. Many studies have shown that radiation can kill

247   tumor cells and promote cell migration and invasion via different mechanisms. It

248   was shown that sublethal X-ray can enhance cell migration(Imaizumi et al., 2018).

249   Another study found that the higher was radioresistance, the higher was the

250   expression of *VEGFR*, which might lead to fast angiogenesis(Lee et al., 2017).

251   "Protein binding" was an important MF-related GO term associated with radiation.

252   As for protein binding, it was reported that the specific binding of *VDR* and *p53* in

253   irradiated HEK 293T was primarily related to cell fate decision(Pemsel et al.,

254   2018).

255   Moreover, KEGG analysis indicated that the MAPK signaling pathway was

256   the most enriched pathway, with 19 related genes. This classic pathway is highly

257   conserved and is involved in many cellular functions, including cell proliferation,

258   differentiation, and migration, which is consistent with the results of GO analysis.

259   A study showed that baseline MAPK signaling activity conferred intrinsic

260   radioresistance to KRAS-mutant colorectal carcinoma cells by rapid up-regulation

261   of *hnRNP K*(Eder et al., 2017). Moreover, quiescent G0 cells were found to be

262   more resistant to ionizing radiation than G1 cells because *P38 MAPK*,

263   *phosphorylated P38 MAPK*, and *RAC2* were regulated in mutual feedback and

264   negative feedback regulatory pathways, leading to the radioresistance of G0

265   cells(Pei et al., 2017). Interestingly, *RPS6KA5, RPS6KA6, CRKL, RAP1A, FASLG,*

266   *and MAPK8* were found in both MAPK and neurotrophin signaling pathway.

267   These genes may be involved in the crosstalk between different signaling

268   pathways, but this hypothesis needs to be tested in further study.

269   Furthermore, in the PPI network analysis, 19 proteins were shown to

270   associated with> 10 other proteins and thus maybe considered as hub proteins in

271   this network. Protein MAPK8 was associated with 10 other proteins and was also

272   found in the MAPK and neurotrophin signaling pathwayin KEGG analysis.

273   Studies on this gene encoding MAPK8 suggest that this kinase plays a key role in

274   T cell proliferation, apoptosis, and differentiation, and may be a crucial protein in

275   cervical cancer radioresistance.

276   In summary, this study determined the profile of differentially expressed

277 circRNAs and their target genes in HeLa cells subjected to radiation. Our results

278 suggest that circRNAs may play a major role in the response to radiation.

279 Considering that only a small percentage of the total circRNA population has been

280 studied to date, the investigation of circRNAs is only beginning. Therefore,

281 additional studies are needed to clarify the importance of circRNAs in the response

282 to radiation and may help elucidate the biological and molecular mechanisms

283 underlying radioresistance in HeLa cells and allow the development of novel

284 therapeutic approaches. The exploration of radioresistance-related circRNAs in

285 radiation-treated HeLa cells may help provide responsive therapy in therapy-

286 resistant cancer and improve prognosis.

287

288 **Acknowledgements:**

289 We thank Professor Jin Shunzi for guiding us about the bioinformatics.

290

291   References:

292   Balkwill, F. 2004. Cancer and the chemokine network. *NATURE REVIEWS CANCER* 4:540-550. 10.1038/nrc1388

293   Burd, C.E., Jeck, W.R., Liu, Y., Sanoff, H.K., Wang, Z., and Sharpless, N.E. 2010b. Expression of linear and novel

294   circular forms of an INK4/ARF-associated non-coding RNA correlates with atherosclerosis risk. *PLoS Genetics*

295   6:e1001233. 10.1371/journal.pgen.1001233

296   de Freitas, A.C., Gomes, L.M.C., and Coimbra, E.C. 2015. Prospects of molecularly-targeted therapies for cervical

297   cancer treatment. *CURRENT DRUG TARGETS* 16:77-91.

298   Du XL, Tao, J., Sheng, X.G., Lu, C.H., Yu, H., Wang, C., Song, Q.Q., Li, Q.S., and Pan, C.X. 2012. Intensity-

299   modulated radiation therapy for advanced cervical cancer: a comparison of dosimetric and clinical outcomes with

300   conventional radiotherapy. *GYNECOLOGIC ONCOLOGY* 125:151-157. 10.1016/j.ygyno.2011.12.432

301   Eder, S., Arndt, A., Lamkowski, A., Daskalaki, W., Rump, A., Priller, M., Genze, F., Wardelmann, E., Port, M., and

302   Steinestel, K. 2017. Baseline MAPK signaling activity confers intrinsic radioresistance to KRAS-mutant colorectal

303   carcinoma cells by rapid upregulation of heterogeneous nuclear ribonucleoprotein K (hnRNP K). *CANCER*

304   *LETTERS* 385:160-167. 10.1016/j.canlet.2016.10.027

305   Ghosh, S., and Krishna, M. 2012b. Role of Rad52 in fractionated irradiation induced signaling in A549 lung

306   adenocarcinoma cells. *Mutat Res* 729:61-72. 10.1016/j.mrfmmm.2011.09.007

307   Imaizumi, H., Sato, K., Nishihara, A., Minami, K., Koizumi, M., Matsuura, N., and Hieda, M. 2018. X-ray-

308   enhanced cancer cell migration requires the linker of nucleoskeleton and cytoskeleton complex. *CANCER SCIENCE*

309   109:1158-1165. 10.1111/cas.13545

310   Ivanov, A., Memczak, S., Wyler, E., Torti, F., Porath, H.T., Orejuela, M.R., Piechotta, M., Levanon, E.Y.,

311   Landthaler, M., Dieterich, C., and Rajewsky, N. 2015. Analysis of intron sequences reveals hallmarks of circular

312   RNA biogenesis in animals. *Cell Reports* 10:170-177. 10.1016/j.celrep.2014.12.019

313   Lee, C., Shim, S., Jang, H., Myung, H., Lee, J., Bae, C.H., Myung, J.K., Kim, M.J., Lee, S.B., Jang, W.S., Lee, S.J.,

314   Kim, H.Y., Lee, S.S., and Park, S. 2017. Human umbilical cord blood-derived mesenchymal stromal cells and small

315   intestinal submucosa hydrogel composite promotes combined radiation-wound healing of mice. *CYTOTHERAPY*

316   19:1048-1059. 10.1016/j.jcyt.2017.06.007

317   Memczak, S., Jens, M., Elefsinioti, A., Torti, F., Krueger, J., Rybak, A., Maier, L., Mackowiak, S.D., Gregersen,

318   L.H., Munschauer, M., Loewer, A., Ziebold, U., Landthaler, M., Kocks, C., le Noble, F., and Rajewsky, N. 2013.

319   Circular RNAs are a large class of animal RNAs with regulatory potency. *NATURE* 495:333-338.

320   10.1038/nature11928

321   Pei, H., Zhang, J., Nie, J., Ding, N., Hu, W., Hua, J., Hirayama, R., Furusawa, Y., Liu, C., Li, B., Hei, T.K., and

322   Zhou, G. 2017. RAC2-P38 MAPK-dependent NADPH oxidase activity is associated with the resistance of

323   quiescent cells to ionizing radiation. *CELL CYCLE* 16:113-122. 10.1080/15384101.2016.1259039

324   Pemsel, A., Rumpf, S., Roemer, K., Heyne, K., Vogt, T., and Reichrath, J. 2018. Tandem Affinity Purification and

325   Nano HPLC-ESI-MS/MS Reveal Binding of Vitamin D Receptor to p53 and other New Interaction Partners in

326   HEK 293T Cells. *ANTICANCER RESEARCH* 38:1209-1216. 10.21873/anticanres.12341

327   Shen, L.F., Zhao, X., Zhou, S.H., Lu, Z.J., Zhao, K., Fan, J., and Zhou, M.L. 2017b. In vivo evaluation of the effects

328   of simultaneous inhibition of GLUT-1 and HIF-1alpha by antisense oligodeoxynucleotides on the radiosensitivity of

329   laryngeal carcinoma using micro 18F-FDG PET/CT. *Oncotarget* 8:34709-34726. 10.18632/oncotarget.16671

330   Zhang, H., Yue, J., Jiang, Z., Zhou, R., Xie, R., Xu, Y., and Wu, S. 2017. CAF-secreted CXCL1 conferred

331   radioresistance by regulating DNA damage response in a ROS-dependent manner in esophageal squamous cell

332   carcinoma. *Cell Death & Disease* 8:e2790. 10.1038/cddis.2017.180

333   Zhao, S., Yao, D.S., Chen, J.Y., and Ding, N. 2013. Aberrant expression of miR-20a and miR-203 in cervical cancer.

334   *Asian Pac J Cancer Prev* 14:2289-2293.

335   Zhong, Y., Du Y, Yang, X., Mo, Y., Fan, C., Xiong, F., Ren, D., Ye, X., Li, C., Wang, Y., Wei, F., Guo, C., Wu, X.,

336   Li, X., Li, Y., Li, G., Zeng, Z., and Xiong, W. 2018. Circular RNAs function as ceRNAs to regulate and control

337   human cancer progression. *Molecular Cancer* 17:79. 10.1186/s12943-018-0827-8

338   **Figure legends**

339 **Figure1. Basic situation of high-throughput sequencing A. Inter–sample**

340 **expression correlation test.** Two groups of HeLa cells were used and each group

341 contained three samples. The cell groups were treated by different methods. The

342 correlation between gene expression levels in different samples indicated the

343 biological repetition. The greater the absolute value of r indicates that the stronger

344 the correlation. **B. CircRNA length distribution.** Approximately 67% of

345 circRNAs had the predicted spliced length of <10,000 nt, whereas 46.4% and 32.0%

346 of the circRNAs had a length of <5,000 and 10,000–50,000 nt, respectively. **C.**

347 **Venn diagram of the differential expression of circRNAs**. The yellow part of

348 the circle is the Control group and the purple part of the circle is the Treatment

349 group.The total number of the circRNAs was 16,893.Approximately 11,456

350 circRNAs were detected in the control group, 11,018 in the treatment group, and

351 5,581 in both groups.**D. Hclusterheatmap.**Hierarchical clustering showing the

352 differential expression profile of circRNAs between the two study groups and the

353 homogeneity within each group.**E.Volcano plot of differentially expressed**

354 **circRNAs.** The green and red dots in the plot represent the differentially expressed

355 circRNAs with statistical significance. The red dots correspond to upregulated

356 circRNAs and the green dots correspond to downregulated circRNAs.**F. circRNA**

357 **genomic feature data**. It shows the novel genomic feature of circRNAs in both

358 groups. Red part is exon, green part is intergenic, blue part is intron.

359 **Figure 2.qRT-PCR results.** The expression patterns of the top four up-regulated

{"1":{"cx":0.11,"cy":0.03}}

360 and top four down-regulated circRNAs as monitored by qRT-PCR. The expression

361 patterns of these eight circRNAs determined byqRT-PCR agreed with the results of

362 the high-throughput sequencing analysis and demonstrated the reliability of the

363 RNA high-throughput sequencing technology.

364 **Figure 3.CircRNA–miRNA–target gene interaction network.** The top four

365 down- and up-regulated circRNAs were used to construct this network using

366 Cytoscape. Putative interactions between miRNAs and circRNAs were evaluated

367 using miRanda. The top five (highest targeting relationship score) miRNAs were

368 selected, then the same miRNAs' target genes were predicted using miRDB.

369 Target scores> 98 were selected.In this figure, rectangles represent mRNAs while

370 the ovals represent circRNAs and triangles represent miRNAs.

371 **Figure 4.Top five GO terms from BP, CC and MF.**The top five GO terms in

372 each group were ranked by p-value. They are peptidyl-tyrosine dephosphorylation;

373 regulation of cell migration; positive regulation of transcription from RNA

374 polymerase II promoter; angiogenesis; morphogenesis of an epithelial sheet(from

375 BP). cell–cell adherens junction; nucleoplasm; cytosol; lamellipodium;

376 nucleus(from CC). protein binding; protein tyrosine phosphatase activity; cadherin

377 binding involved in cell–cell adhesion; RNA polymerase II core promoter

378 proximal region sequence-specific DNA binding; transcriptional activator activity,

379 RNA polymerase II core promoter proximal region sequence-specific binding(from

380 MF).

381 **Figure 5.KEGG analysis.** KEGG pathway analysis was conducted to determine

382 the involvement of target genes in different biological pathways. The size of each

383 circle indicates the number of circRNAs. The color of the circle indicates the p-

384 value. The larger of the circle and the lower of the p-value, the enriched and

385 meaningful of the pathway.

386 **Figure 6.PPI network.** STRING was used to predict protein interactions among

387 the target genes. The interaction scores > 0.9(highest confidence) were selected for

388 constructing PPI networks. The ovals represent proteins with>10 relationships with

389 other proteins and may be the hub proteins in this network.

390

Figure 1

Basic situation of high-throughput sequencing

A. Inter–sample expression correlation test. Two groups of HeLa cells were used and each group contained three samples. The cell groups were treated by different methods. The correlation between gene expression levels in different samples indicated the biological repetition. The greater the absolute value of r indicates that the stronger the correlation. B. CircRNA length distribution. Approximately 67% of circRNAs had the predicted spliced length of <10,000 nt, whereas 46.4% and 32.0% of the circRNAs had a length of <5,000 and 10,000–50,000 nt, respectively. C. Venn diagram of the differential expression of circRNAs. The yellow part of the circle is the Control group and the purple part of the circle is the Treatment group. The total number of the circRNAs was 16,893.Approximately 11,456 circRNAs were detected in the control group, 11,018 in the treatment group, and 5,581 in both groups. D. Hclusterheatmap. Hierarchical clustering showing the differential expression profile of circRNAs between the two study groups and the homogeneity within each group. E. Volcano plot of differentially expressed circRNAs. The green and red dots in the plot represent the differentially expressed circRNAs with statistical significance. The red dots correspond to upregulated circRNAs and the green dots correspond to downregulated circRNAs.F. circRNA genomic feature data. It shows the novel genomic feature of circRNAs in both groups. Red part is exon, green part is intergenic, blue part is intron.

Pearson correlation between samples
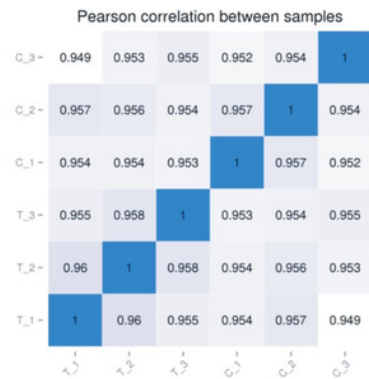
A
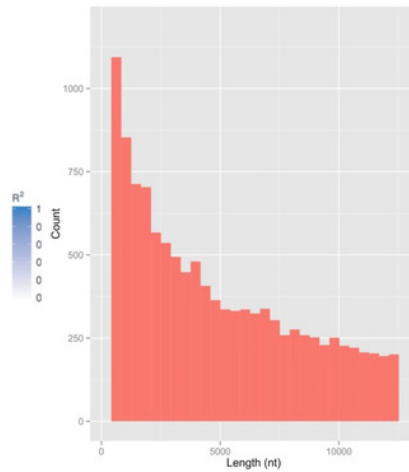
B

C
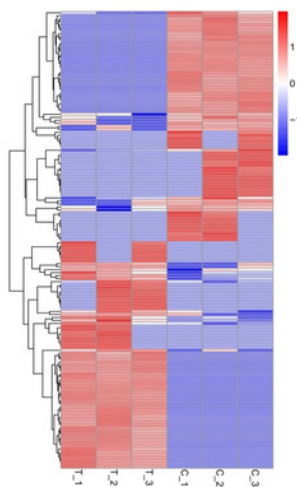
D
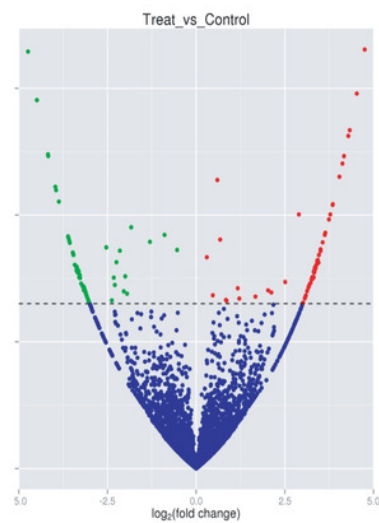
E
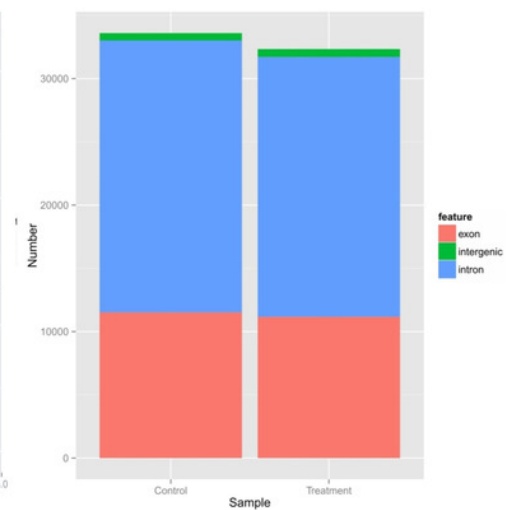
F

Figure 2

qRT-PCR results

The expression patterns of the top four up-regulated and top four down-regulated circRNAs as monitored by qRT-PCR. The expression patterns of these eight circRNAs determined by qRT-PCR agreed with the results of the high-throughput sequencing analysis and demonstrated the reliability of the RNA high-throughput sequencing technology.
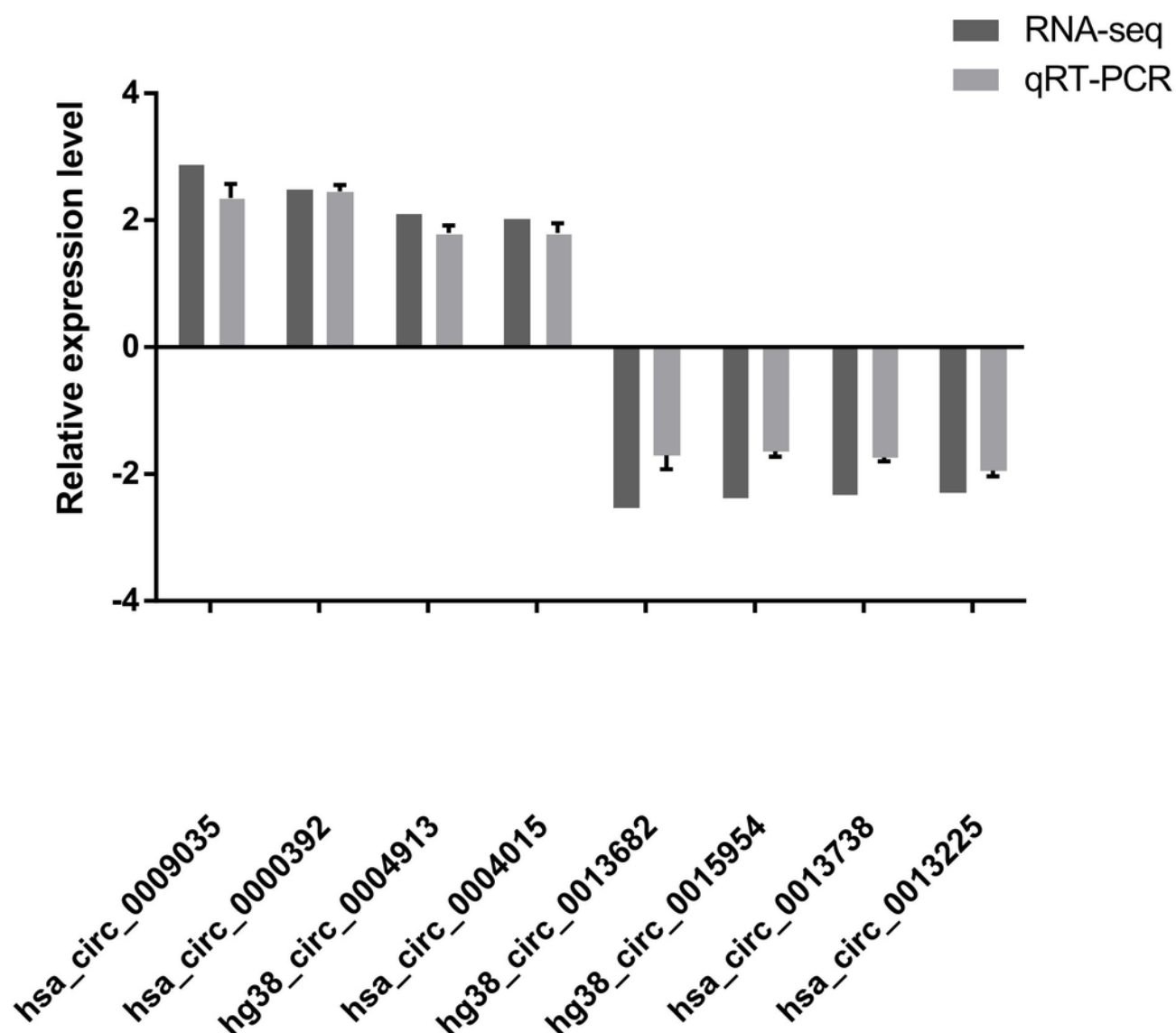
Figure 3

CircRNA–miRNA–target gene interaction network

The top four down- and up-regulated circRNAs were used to construct this network using Cytoscape. Putative interactions between miRNAs and circRNAs were evaluated using miRanda. The top five (highest targeting relationship score) miRNAs were selected, then the same miRNAs' target genes were predicted using miRDB. Target scores> 98 were selected.In this figure, rectangles represent mRNAs while the ovals represent circRNAs and triangles represent miRNAs.
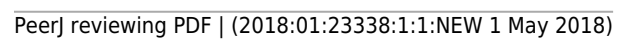
Figure 4

Top five GO terms from BP, CC and MF

The top five GO terms in each group were ranked by p-value. They are peptidyl-tyrosine dephosphorylation; regulation of cell migration; positive regulation of transcription from RNA polymerase II promoter; angiogenesis; morphogenesis of an epithelial sheet (from BP). cell–cell adherens junction; nucleoplasm; cytosol; lamellipodium; nucleus (from CC). protein binding; protein tyrosine phosphatase activity; cadherin binding involved in cell–cell adhesion; RNA polymerase II core promoter proximal region sequence-specific DNA binding; transcriptional activator activity, RNA polymerase II core promoter proximal region sequence-specific binding (from MF).
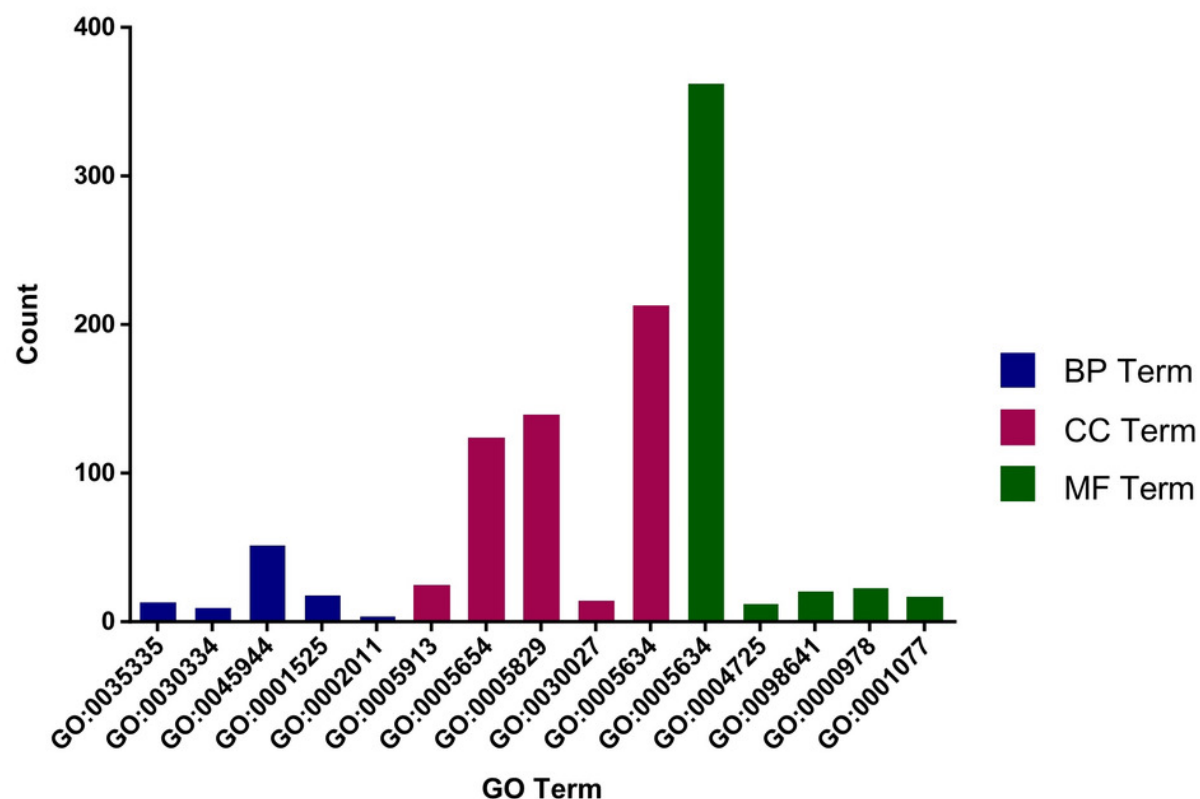
Figure 5

KEGG analysis

KEGG pathway analysis was conducted to determine the involvement of target genes in different biological pathways. The size of each circle indicates the number of circRNAs. The color of the circle indicates the p-value. The larger of the circle and the lower of the p-value, the enriched and meaningful of the pathway.

pathway enrichment
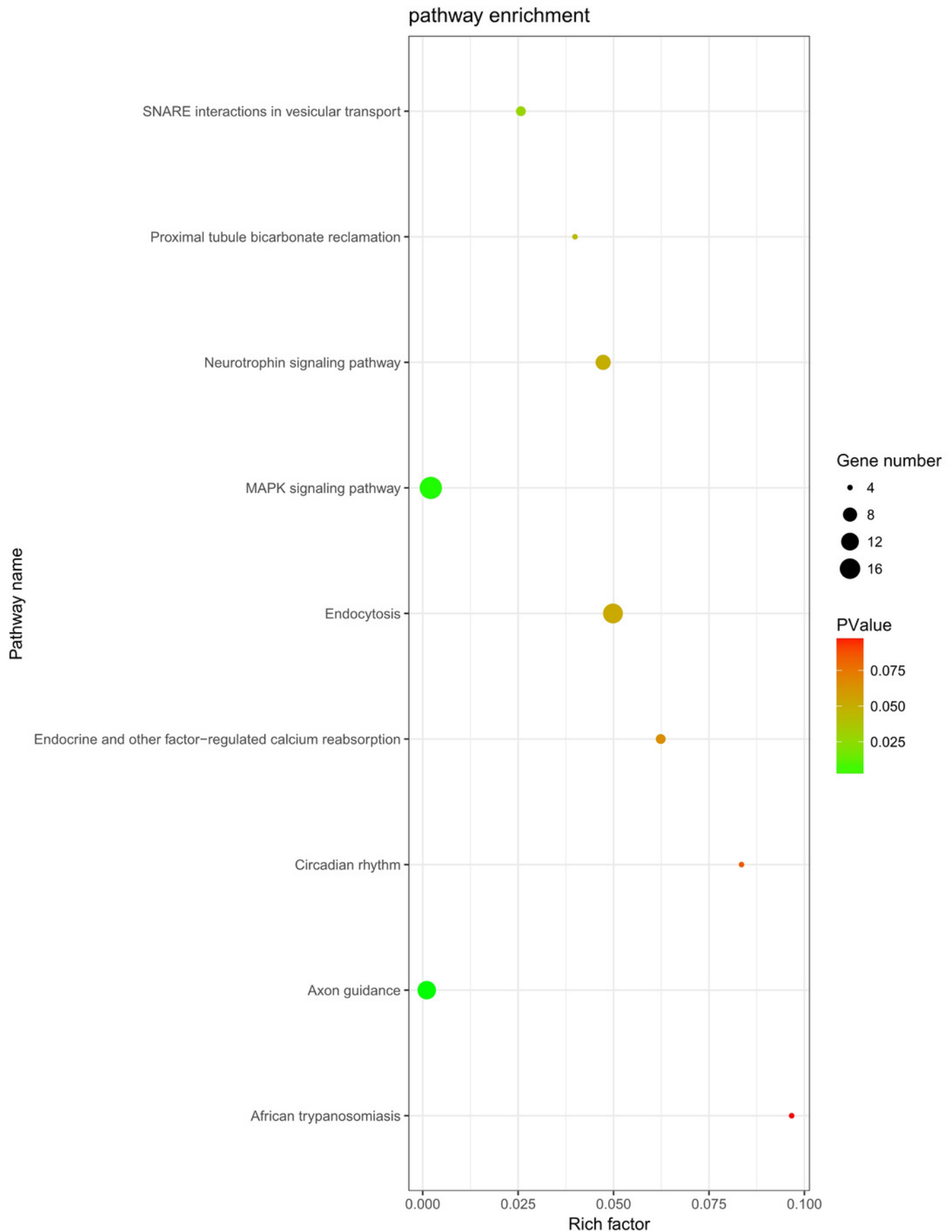
Figure 6

PPI network

STRING was used to predict protein interactions among the target genes. The interaction scores > 0.9 (highest confidence) were selected for constructing PPI networks. The ovals represent proteins with>10 relationships with other proteins and may be the hub proteins in this network.
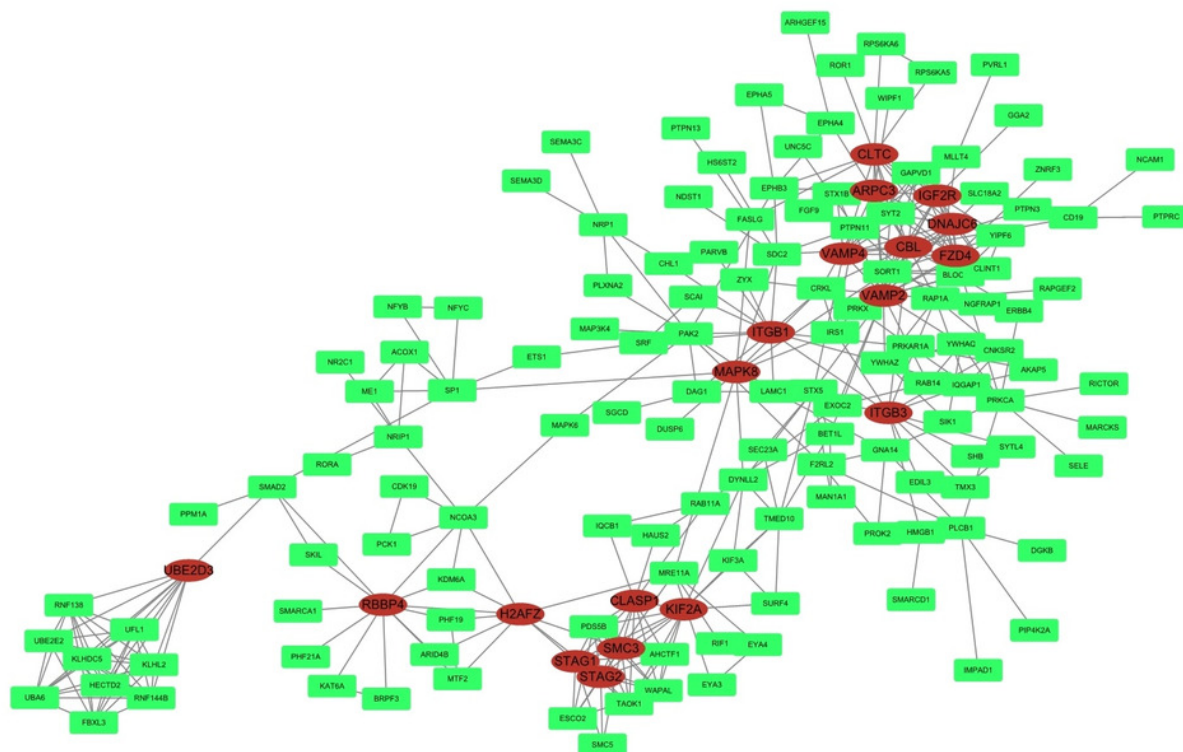
Primers used in qRT-PCR

1 Table 1 primers used in qRT-PCR

Gene	Forward primer (5′ to 3′)	Reverse primer (5′ to 3′)	Variation tendency
Gapdh	TGACTTCAACAGCGACA CCCA	CACCCTGTTGCTGTAGC CAAA	
hg38_circ_00136 82	GGCAGACAGAAGGAAA CAGC	GCTTTTGCTCTTGGGTTC TG	down-regulated
hg38_circ_00159 54	CAAGGACTGCCTGATTG ACAAG	GGAGGTGAGGGAGGA GTTCA	down-regulated
hsa_circ_001373 8	TCCTTCCTGCCTTTAACA CAC	TGGTAGCACCCATTTGT GAA	down-regulated
hsa_circ_001322 5	CCGGACACTTGTTTTCC AGT	TTCTGTTTGTGAGCAAT CATCC	down-regulated
hg38_circ_00049 13	CTGCCATAGGACAGGCT GA	GGCACAAAGACAGCCTA ATGA	up-regulated
hsa_circ_000903 5	TTAGGTGGTTGAGCGCC TGC	GGGCAGTTCACCAACAGCTT	up-regulated
hsa_circ_000039 2	ACAGAAGGGCAAGAGA GGTGG	TTCCTTGGTCCTCGAGG CAC	up-regulated
hsa_circ_000401	AGGGGAAGGATCTTAT	CACTGAGTCCATTCCCT	up-

| 5 | GCTACAGT | GGCA | regulated |

The top five (ranked by p-value) BP terms, CC terms, and MF terms

1   Table 2. The top five(ranked by p-value) BP terms, CC terms, and MF terms

GO	*P*-value	Description	GO terms
GO:0035335	1.20E-04	peptidyl-tyrosine dephosphorylation	biological_process
GO:0030334	8.18E-04	regulation of cell migration	biological_process
GO:0045944	0.0013274	positive regulation of transcription from RNA polymerase II promoter	biological_process
GO:0001525	0.0014863	angiogenesis	biological_process
GO:0002011	0.0018697	morphogenesis of an epithelial sheet	biological_process
GO:0005913	1.67E-04	cell-cell adherens junction	cellular_component
GO:0005654	2.11E-04	nucleoplasm	cellular_component
GO:0005829	7.43E-04	cytosol	cellular_component
GO:0030027	7.79E-04	lamellipodium	cellular_component
GO:0005634	9.11E-04	nucleus	cellular_component
GO:0005515	6.07E-10	protein binding	molecular_function
GO:0004725	4.76E-04	protein tyrosine phosphatase activity	molecular_function
GO:0098641	0.001694	cadherin binding involved in cell-cell adhesion	molecular_function
GO:0000978	0.003848	RNA polymerase II core promoter proximal region sequence-specific DNA binding	molecular_function
GO:0001077	0.005654	transcriptional activator activity, RNA polymerase II core promoter proximal region sequence-specific binding	molecular_function

The top five (ranked by gene count) KEGG pathways

1   Figure 3. The top five(ranked by gene count) KEGG pathways

Term	Count	PValue	Genes
MAPK signaling pathway	19	0.002114	PRKCA, FGF9, TAOK1, NLK, PPM1A, FASLG, PPM1B, STK4, SRF, RPS6KA5, RPS6KA6, MAP3K4, CRKL, PAK2, RASGRP3, RAP1A, MAPK8, RAPGEF2, DUSP6
Endocytosis	15	0.049837	PARD6B, ERBB4, KIF5C, CBL, ASAP2, EEA1, SMAD2, PSD2, CLTC, ARPC3, IGF2R, KIAA1033, DNAJC6, RAB11A, WIPF1
Axon guidance	13	0.00105	EPHA5, ABLIM1, EPHA4, NRP1, PAK2, SEMA6D, PLXNA2, ABLIM3, SEMA3D, SEMA3C, UNC5C, EPHB3, ITGB1
Neurotrophin signaling pathway	9	0.047261	RPS6KA5, RPS6KA6, CRKL, RAP1A, SORT1, FASLG, MAPK8, IRS1, PTPN11
SNARE interactions in vesicular transport	5	0.025713	STX5, VAMP4, BET1L, VAMP2, STX1B
Endocrine and other factor-regulated calcium reabsorption	5	0.06235	PRKCA, KL, RAB11A, CLTC, PLCB1
Proximal tubule bicarbonate reclamation	4	0.039887	SLC38A3, GLS, GLUD1, PCK1
Circadian rhythm	4	0.083514	CRY2, BHLHE40, RORA, FBXL3
African trypanosomiasis	4	0.096652	PRKCA, FASLG, PLCB1, SELE